ORGANOMETALLICS

Article

Cite This: *Organometallics* XXXX, XXX, XXX−XXX

pubs.acs.org/Organometallics

Synthesis and Study of a Dialkylbiaryl Phosphine Ligand; Lessons for Rational Ligand Design

Dillon J. Bryant, Lev N. Zakharov, and David R. Tyler*

Department of Chemistry and Biochemistry, University of Oregon, 1253 University of Oregon, Eugene, Oregon 97403, United States

Supporting Information

ABSTRACT: The rational design and synthesis of a novel dialkylbiarylphosphine ligand, 2′-(dimethylphosphine)-2,6-dimethoxy-1,1′-biphenyl (MeSPhos), for palladium-catalyzed C−N cross-coupling reactions is described. Based on previous results, it was hypothesized that a ligand with electronic properties similar to (2-biphenyl)dimethylphosphine (MeJPhos) but with greater steric bulk would allow the cross-coupling of previously inaccessible deactivated aryl chlorides. As predicted, MeSPhos exhibited similar electronic properties to MeJPhos. However, MeSPhos surprisingly showed a significantly smaller steric profile than MeJPhos. In comparison to the widely used CySPhos (2-dicyclohexylphosphino-2′,6′-dimethoxybiphenyl), MeSPhos promoted the oxidative addition of highly deactived aryl chlorides for which CySPhos was ineffective, but significantly decreased the rate of reductive elimination. The kinetics of cross-coupling reactions showed that the altered steric and electronic parameters of MeSPhos had a significant impact on the rate of cross-coupling, and the decreased steric bulk had a profound deleterious impact on the catalyst stability. With regard to this latter point, only the most activated aryl chlorides reacted at a sufficient rate to overcome the rate of catalyst decomposition. These results indicate that the relationship between the electron-donating ability of the phosphine ligand and the rate of oxidative addition is complex, and they also illustrate that increasing substitution on the biphenyl structure does not necessarily increase the steric bulk of the ligand.

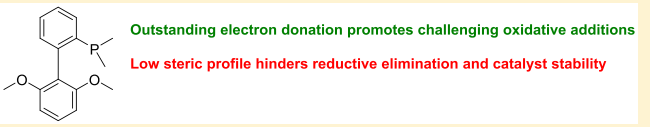

INTRODUCTION

Carbon−nitrogen bond-forming reactions are of keen interest for applications in medicine and biotechnology.[1] Despite the ubiquity of C−N bonds in biologically relevant molecules, the synthetic toolkit for achieving these transformations is limited.[2] Among the C−N bond-forming reactions, the Buchwald-Hartwig cross-coupling has become a preeminent tool for the formation of aryl C−N bonds (Figure 1).[3,4]

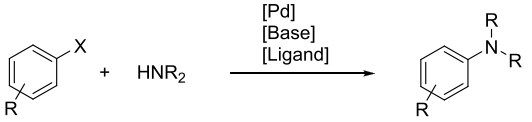

Figure 1. General form of a Buchwald-Hartwig C−N cross-coupling reaction.

Despite the development of multiple phosphine ligands (Figure 2) for these cross-coupling transformations, significant challenges remain. For instance, many pharmaceutical targets include sterically hindered amines or would involve the cross-coupling of heteroaryl chlorides—two notoriously difficult classes of cross-coupling partners.[1,5,6] Likewise, highly deactived aryl chlorides present significant difficulties as starting materials because they are significantly less active than their bromide and triflate counterparts, frequently requiring strenuous conditions that may not be compatible with highly functionalized molecules.[6]

A successful ligand must have two key properties to expedite the possible rate-limiting steps in the catalytic mechanism (Figure 3): (1) it must donate sufficient electron density to the palladium center in the catalyst to facilitate rapid oxidative addition of the substrate, and (2) it must be sufficiently sterically bulky to facilitate reductive elimination of the arylamine.[7] Past work by Hartwig and co-workers has shown that for Pd^0L_2 species the mechanism of oxidative addition depends only on the identity of the aryl halide and is unaffected by the steric bulk of the ligand.[8] It is not clear, however, if this pattern holds for the Pd^0L_1 species that are generated by Buchwald-type precatalysts.[9] An additional feature of the later-generation dialkylbiaryl phosphine ligands is the *para*-substitution on the nonphosphine containing ring; this substitution allows a Pd-OR interaction which stabilizes oxidative addition complexes.[10] In addition, the ligand must sufficiently shield the Pd center to prevent metallic aggregation and decomposition.[11]

Although palladium catalyzed C−N bond-forming reactions were initially developed using phosphine ligands, recent work has shown that other types of ligands are also effective partners for these transformations, predominantly *N*-heterocyclic carbene (NHC) ligands and more rarely exotic ligands such as ylides.[12−14] Beller-type ligands, based on a dialkylphosphinoimidazole scaffold, have also proven to be highly effective

Received: March 7, 2019

DOI: 10.1021/acs.organomet.9b00153
Organometallics XXXX, XXX, XXX−XXX

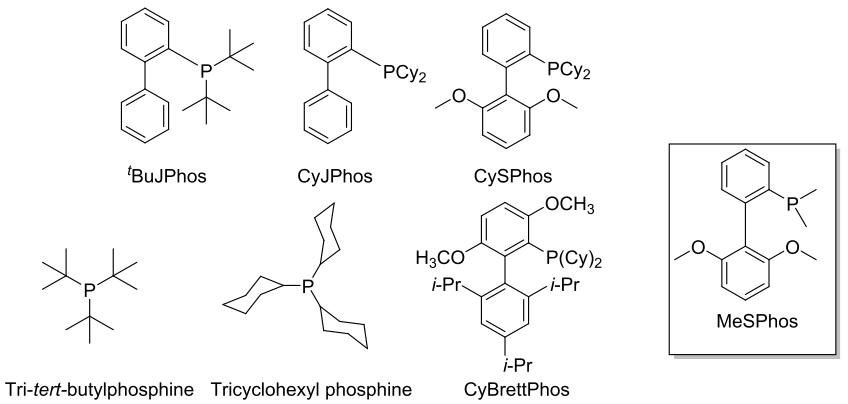

Figure 2. Common phosphine ligands used in aryl amination reactions.

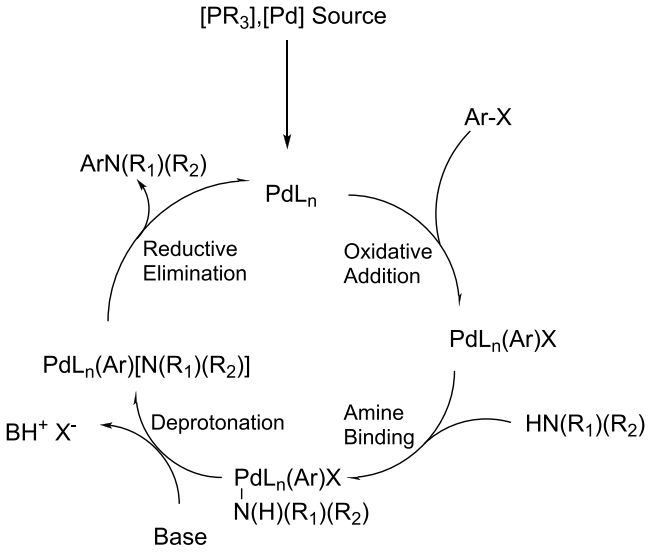

Figure 3. Proposed cycle for Pd-catalyzed C−N cross-coupling reactions.

ligands, particularly for the synthesis of important pharmaceutical targets.[15,16] In addition, the use of bidentate phosphine ligands frequently has several advantages such as lower catalyst loadings and improved turnover numbers.[17]

With these properties in mind, we sought to rationally design a phosphine ligand capable of catalyzing the amination of deactivated aryl chlorides. Using structure−activity relationships and reactivity data from our previous studies,[18,19] we hypothesized that MeSPhos (2′-(dimethylphosphine)-2,6-dimethoxy-1,1′-biphenyl) would be capable of cross-coupling highly deactived aryl chlorides based on two factors: (1) The σ-donating ability of the RJPhos ligands follow the trend ^{t}BuJPhos < EtJPhos < ^{i}PrJPhos < CyJPhos ≪ MeJPhos.[19] It is reasonable to predict a similar trend with the RSPhos ligands. If so, the strong electron-donating ability of the MeSPhos ligand should promote oxidative addition. (2) Methoxy substitution on the biphenyl scaffold will increase the steric bulk of the ligand, thereby promoting reductive elimination and increasing catalyst stability. We report herein the synthesis of MeSPhos, a rationally designed ligand intended to promote both oxidative addition and reductive elimination, either of which could be the rate-limiting step in the catalytic cycle. In addition, we report the results of using the MeSPhos ligand in C−N cross-coupling reactions.

RESULTS AND DISCUSSION

Synthesis of MeSPhos (4). MeSPhos was synthesized in four steps from commercially available reagents (Figure 4). 1,3-Dimethoxybenzene was treated sequentially with *n*-butyllithium and 1,2-dibromobenzene to yield 2′-bromo-2,6-dimethoxybiphenyl (**1**) in good yields (70−80%). Subsequent treatment with *n*-butyllithium and diethyl chlorophosphate yielded phosphonate **2** in good yield (70−80%). The reaction of **2** with methylmagnesium bromide and sodium triflate,

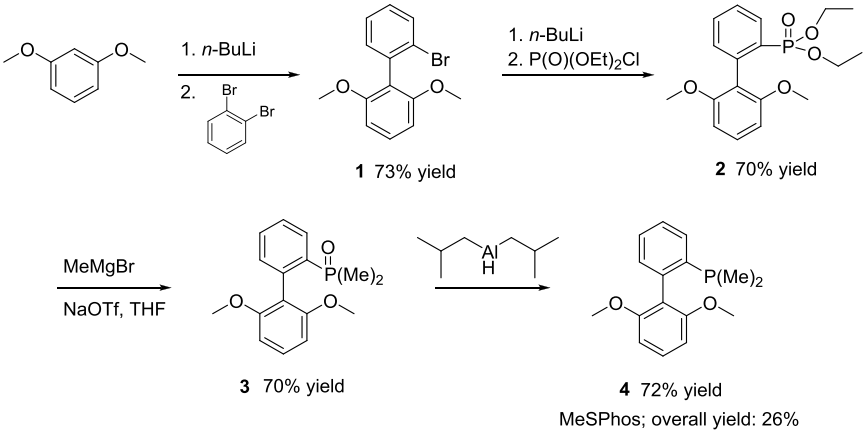

Figure 4. Synthesis of MeSPhos (**4**) from commercially available precursors.

DOI: 10.1021/acs.organomet.9b00153
Organometallics XXXX, XXX, XXX−XXX

reported recently by our group,[20] yielded the phosphine oxide **3**. Reduction of the phosphine oxide with diisobutylaluminum hydride (DIBAL-H), using a method reported by us,[21] yielded MeSPhos (**4**) in 26% overall yield.

Electronic Characterization of MeSPhos. To quantify the electronic properties of the MeSPhos ligand, the $Cr(CO)_5PR_3$ complexes in Table 1 were synthesized and their infrared spectra analyzed. The CO absorbance bands of the complexes were identified based on prior studies (Table 1),[18] and the relative vibrational force constants were calculated from the appropriate frequencies.[22] The force constants are summarized in Table 1. From these results, the σ-basicities and π-acidities of MeSPhos and CySPhos relative to ^{t}BuJPhos were calculated using the Graham treatment (eqs 1 and 2).[22−24]

Table 1. Band Frequencies and Force Constants of the $Cr(CO)_5PR_3$ Complexes[a]

Phosphine	^{t}BuJPhos[18]	MeJPhos[18]	MeSPhos	CySPhos	CyJPhos[18]
ν_1(A1)	2072.1	2059.6	2060.9	2073	2072.1
ν_2(B1)	2062.5	2003.2	1979.2	2058	2056.7
ν_3(E)	1937.1	1937.5	1937.27	1937	1937.1
k_i	1.0127	0.52276	0.33134	0.97526	0.96446
k_1	15.828	15.507	15.377	15.153	15.796
k_2	17.178	16.205	15.819	17.104	17.082

[a] k_i is the force constant for CO−CO interactions, k_1 is the stretching force constant for the CO *trans* to the phosphine, and k_2 is the stretching force constant for the CO group *cis* to the phosphine.[18] All force constants in mdyn/Å. All frequencies in cm^{-1}.

As shown in Table 2, the $\Delta\pi$ and $\Delta\sigma$ values of MeSPhos are modestly changed relative to the values for MeJPhos ($\Delta\pi$: −3.64% vs −5.06%; $\Delta\sigma$: 9.31% vs 12.98%; all values normalized relative to ^{t}BuJPhos). These results indicate that the methyl groups' electronic properties are largely retained despite alteration of the biphenyl scaffold. Similarly, there is almost no difference in the electronic properties between CySPhos and CyJPhos ($\Delta\pi$: 0.0382% vs −0.00359%; $\Delta\sigma$: −0.0339% vs 0.00920%; all values normalized relative to ^{t}BuJPhos), indicating that, as hypothesized, electronic effects are dominated by the substituents at phosphorus and relatively unaffected by substitutions on the biphenyl scaffold.

Table 2. Relative σ Donation and π Acceptance of the $Cr(CO)_5PR_3$ Complexes Relative to ^{t}BuJPhos[a]

Phosphine	^{t}BuJPhos	MeJPhos	MeSPhos	CySPhos	CyJPhos
Δk_i	0	0.3203	0.4511	0.6751	0.0321
Δk_2	0	0.974	1.356	0.0749	0.0965
$\Delta\sigma$	0	1.63	−2.268	−0.525	−0.1609
$\Delta\pi$	0	−0.653	0.909	0.6002	0.0644
$\Delta\sigma$(%)	0	9.31	12.98	−0.0339	0.00920
$\Delta\pi$(%)	0	−3.64	−5.06	0.0382	−0.00359

[a] k_1 and k_2 in mdyne/Å. See the SI for details on how these parameters were calculated.

$$\Delta k_1 = \Delta\sigma + 2\Delta\pi \quad (1)$$

$$\Delta k_2 = \Delta\sigma + \Delta\pi \quad (2)$$

Steric Characterization of MeSPhos. The steric profile of MeSPhos was studied by synthesizing (Figure 5) and crystallizing (Figure 6) the *trans*-$Pd(MeSPhos)_2Cl_2$ complex and then comparing the structure to the known X-ray structures of the *trans*-$Pd(PR_3)_2Cl_2$ complexes, where PR_3 is CySPhos, CyJPhos, and MeJPhos. The steric data are summarized in Table 3. From these data, several interesting conclusions can be drawn. As shown in prior work, the palladium−phosphine distance is a proxy for front-strain induced by the ligand.[18] As expected, CyJPhos exhibits significantly higher front strain than MeJPhos (longer Pd−P bond length: 2.380 Å vs 2.319 Å, respectively). However, replacement of the cyclohexyl groups on the SPhos scaffold with methyl groups changes the Pd−P bond length only slightly (2.349 Å for cyclohexyl and 2.342 Å for methyl), a difference far less than the difference between MeJPhos and CyJPhos (2.319 and 2.380 Å, respectively). This suggests that in the SPhos scaffold front strain is governed heavily by substitution on the biphenyl ring and only slightly by substitution at phosphorus. This counterintuitive conclusion likely arises from a simple observation of the crystal structures: in the unsubstituted ligands (MeJPhos and CyJPhos), the nonphosphorus containing phenyl ring is oriented toward the palladium, while in the methoxy-substituted ligands (MeSPhos and CySPhos), the nonphosphorus-containing phenyl ring is oriented away from the palladium. This phenomenon is related to the biphenyl torsional angle, a factor that will be discussed in more depth in the following paragraphs. This ligand−palladium interaction would best be described as back-strain; however, it shows how these measures of steric bulk often affect one another and are deeply interrelated.

The percent buried volume (Table 3) is a measure of the overall steric profile that incorporates front strain but also considers all steric contributions of atoms within a 3.5 Å sphere centered at palladium. This parameter was calculated using SambVca 2, an online tool developed by Falivene et al.[25] Two important points come out of the percent buried volume calculations: (1) As chemical intuition would predict, CySPhos is slightly larger than CyJPhos (32.7% versus 32.1%, respectively), but the difference is relatively small. This point is important because it hints that substitution on the biaryl scaffold has only a modest impact on the steric bulk of the ligand. (2) As also expected, MeJPhos is smaller than CyJPhos (30.5% versus 32.1%, respectively) but the difference is only 5%. In contrast, the difference between MeSPhos, 26.7% buried volume, and CySPhos, 32.7% buried volume, is 18%, significantly larger than would be anticipated based on the

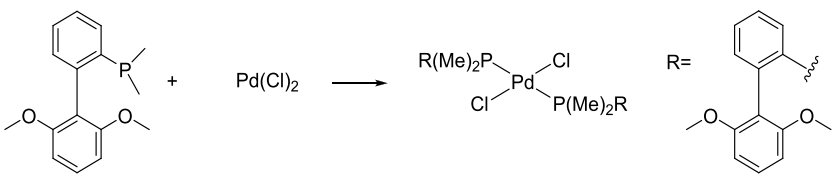

Figure 5. Synthesis of *trans*-$(MeSPhos)_2PdCl_2$.

DOI: 10.1021/acs.organomet.9b00153
Organometallics XXXX, XXX, XXX−XXX

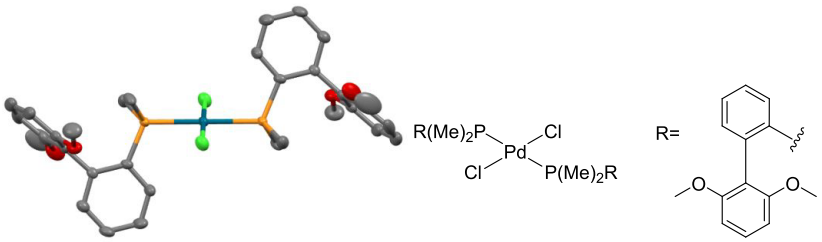

Figure 6. ORTEP crystal structure of $PdCl_2(MeSPhos)_2$. Thermal ellipsoids are drawn at 50% probability. Hydrogens have been omitted for clarity.

Table 3. Summary of Steric Data Comparing MeSPhos to the Previously Reported MeJPhos and the Commercially Available CyJPhos and CySPhos[a]

Parameter	CyJPhos[27]	CySPhos[28]	MeSPhos	MeJPhos[18]
Pd–P bond length (Å)	2.380	2.349	2.342	2.319
Percent buried volume (including hydrogens) (%)	32.1	32.7	26.7	30.5
Symmetric deformation coordinate, S4′	16.91	9.97	18.34	27.96

[a]All data are from the *trans*-$Pd(PR_3)_2Cl_2$ complexes with the exception of CyJPhos, which was obtained from the *trans*-$Pd(PR)_3Br_2$ complex.

small difference in MeJPhos and CyJPhos (Table 3). Careful examination of the crystal structure provides a possible explanation for why the difference between MeSPhos and CySPhos is so large; specifically, CySPhos exhibits a biphenyl torsional angle of 89.90°, whereas MeSPhos exhibits a biphenyl torsional angle of 82.93°. (For comparison, the biphenyl torsional angles in MeJPhos and CyJPhos are 59.24° and 61.82°, respectively. See Figure S1 in the Supporting Information for a graphic representation of the biphenyl torsional angles and how they were calculated.) These data suggest that for the SPhos scaffold, the overall steric bulk is dictated primarily by substitution at phosphorus and only secondarily by substitution on the biphenyl ring—likely because the methoxy-containing ring is oriented away from the palladium, and only a sparing number of hydrogen atoms are within the 3.5 Å sphere considered by the percent buried volume calculation.

The last steric parameter discussed is the symmetric deformation coordinate, S4′,[26] which describes the distortion at phosphorus in a metal complex from tetrahedral geometry (high S4′, low steric demand) to trigonal pyramidal geometry (near-zero or negative S4′, high steric demand). For a graphic explaining the S4′, see Figure S2 in the Supporting Information. As expected, cyclohexyl substitution at phosphorus leads to a significantly lower S4′ than methyl substitution (9.97 for CySPhos and 18.34 for MeSPhos), strongly suggesting that substitution at phosphorus profoundly alters the sterics of phosphines coordinating to metal centers. However, it is noteworthy that CyJPhos and CySPhos also have significantly different S4′ values (16.91 and 9.97, respectively), which indicates that the coordination geometry at phosphorus is also affected by the substitution on the biphenyl scaffold. The point here is that substitution at phosphorus and substitution on the biphenyl scaffold can both affect the S4′ value, which has a direct impact on the steric demand of the ligand.

Taken together, these steric results illustrate an important point: the steric properties of a ligand cannot be adequately described by any single parameter because back-strain, front-strain, and overall volume often trend together but do not necessarily depend on one another. Given these results, our hypothesis that MeSPhos will exhibit a greater steric strain than MeJPhos was incorrect; in fact, MeSPhos has the smallest overall steric profile (percent buried volume = 26.7%), despite having the second shortest Pd–P bond length (2.342 Å). Thus, our second hypothesis proposed in the Introduction, that methoxy substitution on the biphenyl scaffold will increase steric bulk, is not supported by these data.

Reactivity of MeSPhos in Pd-Catalyzed C–N Cross-Coupling Aminations. C–N cross-couplings involving MeSPhos and Pd^0 salts were studied. Unfortunately, the only aryl chloride substrate for which catalytic amination reactivity could be reproducibly demonstrated was *p*-chlorobenzonitrile, a highly activated aryl chloride (Figure 7). Analysis of the failed reactions showed that in most cases, the majority of the aryl chloride simply failed to react; however, in some cases we observed a small amount of the dehalogenated product, a known product of catalyst decomposition and failed reductive elimination.[5] In a single case, we observed catalytic conversion of the aryl chloride to the dehalogenated product in approximately 20% yield (Figure 8).[29,30] (See section 1 of the Supporting Information for the full list of substrates studied and the reaction conditions.) It was hypothesized that the low reactivity was due to failed generation of the

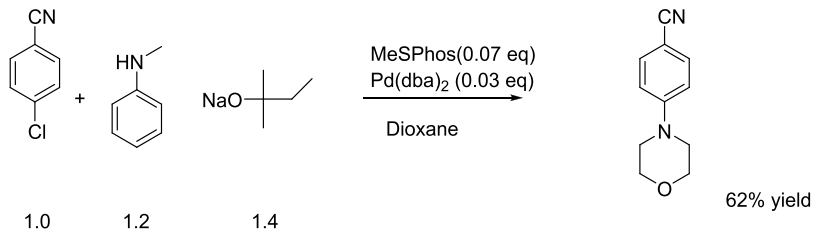

Figure 7. Cross-coupling of *p*-chlorobenzonitrile with morpholine. Yield is based on duplicate runs and estimated based on ^1H NMR spectra.

DOI: 10.1021/acs.organomet.9b00153
Organometallics XXXX, XXX, XXX–XXX

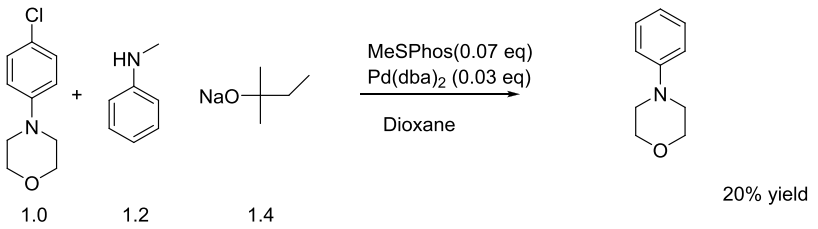

Figure 8. Catalytic dehalogenation of 4-(4-chlorophenyl)morpholine was observed as a major side product during the corresponding C–N cross-coupling reaction. Yield is estimated based on ^{1}H NMR spectra and recovered mass.

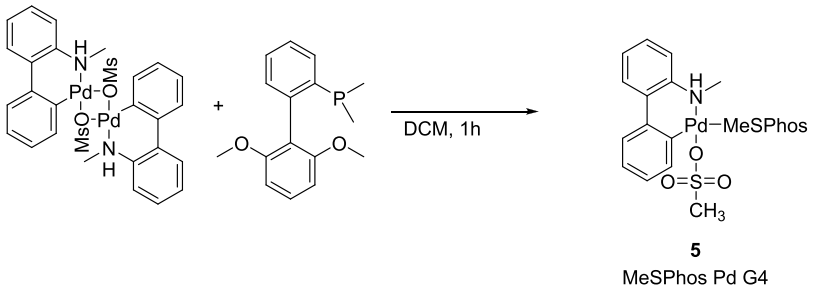

Figure 9. Synthesis of the generation 4 (G4) precatalyst from the free phosphine.

catalytically active species (Figure 3), which is a well-known challenge in Pd cross-coupling reactions.[29,31,32] In an attempt to increase the generation of a more active catalytic species, precatalyst **5** (Figure 9) was synthesized based on Buchwald's N-substituted aminobiphenyl palladium system (Figures 9 and 10).[9,33]

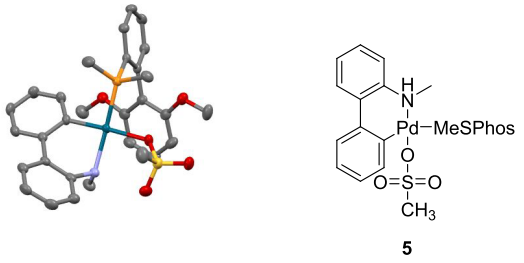

Figure 10. ORTEP crystal structure of MeSPhos Pd G4, **5**. Thermal ellipsoids are drawn at 50% probability. Hydrogens have been omitted for clarity.

Unfortunately, precatalyst **5** exhibited nearly identical reactivity to the free phosphine/Pd^{0} catalyst system. (See section 1 of the Supporting Information for details and full reaction screenings.) In light of these results, two possibilities were considered: (1) MeSPhos was forming an active catalytic species, but the active catalytic species decomposed relatively quickly so that only highly activated aryl chlorides could be successfully aminated; or (2) MeSPhos was incapable of oxidatively adding deactivated aryl chlorides.

Attempted Isolation of the Oxidative-Addition Complex with Griseofulvin. To differentiate between the hypotheses presented in the previous paragraph, griseofulvin, an extremely deactivated aryl chloride, was selected as the substrate. The synthesis and crystallization of the MeSPhos·Pd·griseofulvin oxidative addition complex was repeatedly attempted, but no stable product was obtained. (As shown in Figure 3, the amine has no role in the oxidative addition step. Therefore, no amine was included in these reactions.) However, ^{1}H, ^{13}C, and ^{31}P NMR spectroscopy provided strong evidence for the formation of the oxidative addition complex (Figure 11 and section 5 in the Supporting Information). Prior studies showed that significant downfield shifts occur in the ^{31}P NMR spectra when oxidative addition occurs.[10,34] For example, the free CySPhos ligand resonates at −8.6 ppm in the ^{31}P NMR spectrum, whereas the oxidative addition complex with chlorobenzene has resonances at ca. 35 ppm (Δppm = 44).[28,34] For MeSPhos, the free ligand resonates at −54 ppm, and the resonance attributed to the oxidative addition product is at −8.5 ppm (Δppm = 46 ppm). In addition, ^{13}C/^{1}H NMR HMBC and 1-dimensional NOSEY experiments showed through-space interactions of the MeSPhos with protons on griseofulvin, indicating that the MeSPhos and griseofulvin are within approximately 6 Å (see section 5 of the Supporting Information for details). This NMR evidence and the evidence for a palladium bound phosphine are interpreted as strong evidence that MeSPhos supports the rapid oxidative addition of highly deactivated aryl chlorides, but the resulting complex is relatively unstable, decomposing in less than 4 h at room temperature. Thus, the second hypothesis in the previous paragraph, that MeSPhos was incapable of oxidatively adding deactivated aryl chlorides, is refuted by these data. In contrast, using NOESY experiments, we found no evidence that CySPhos promoted the oxidative addition of griseofulvin (Figures S50–S52). These results imply that the electron-donating ability of the phosphine may have an effect on the ability of its palladium complexes to undergo oxidative addition.

Kinetics and Reactivity Studies. Based on the hypotheses presented in the Introduction,[5] we expected the excellent electron-donating ability of MeSPhos to promote oxidative addition at a far faster rate than the comparable CySPhos, which is less electron-donating. However, plots of concentration vs time (Figures S22–S25) for the oxidative addition reactions using these ligands do not support this hypothesis (see SI section 8).[35] More specifically, the data in SI section 8 show the following: (1) Either MeSPhos promotes oxidative addition more slowly than CySPhos, or the oxidative addition product undergoes rapid decomposition (CySPhos rapidly

DOI: 10.1021/acs.organomet.9b00153
Organometallics XXXX, XXX, XXX–XXX

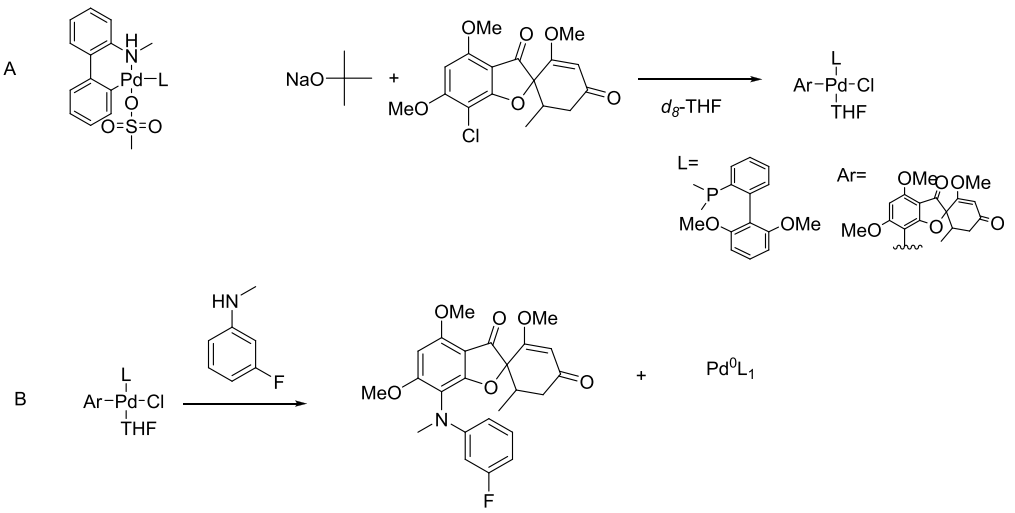

Figure 11. Stepwise cross-coupling of griseofulvin with 3-fluoro-*N*-methylaniline using the MeSPhos Pd G4 precatalyst.

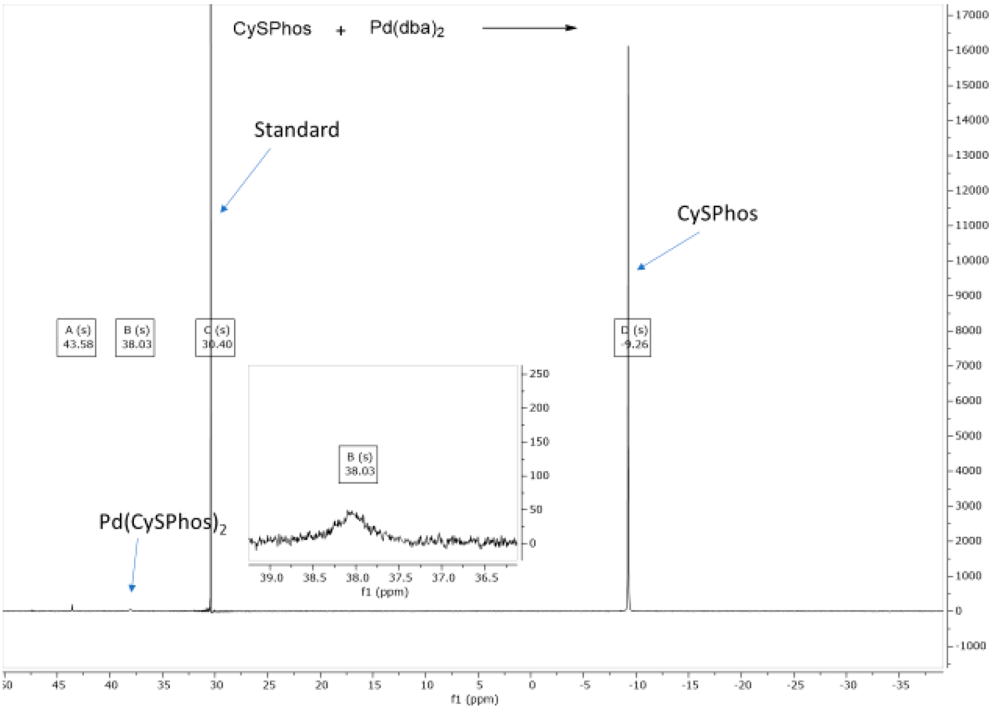

Figure 12. ^{31}P $\{^1H\}$ NMR spectrum of the reaction between CySPhos and $Pd(dba)_2$ in dioxane. The broad singlet at ca. 38 ppm is likely the $Pd(CySPhos)_2$,[37] and we hypothesize that the peak at ca. 44 is the Pd(CySPhos) complex.

forms a stable oxidative addition product); (2) under standard cross-coupling conditions involving Pd^0 salts and precatalysts, multiple catalytically active species are present, as discussed next.[36]

An additional complication in the interpretation of the kinetics data was the presence of multiple catalytically active species. Prior work established that multiple catalytically active species form in the oxidative addition of aryl bromides, but only a single species is active for aryl chlorides. To probe the presence of multiple catalytically active species, we studied the reaction of $Pd(dba)_2$ and MeSPhos or CySPhos in the absence of an aryl chloride using ^{31}P NMR spectroscopy. For both MeSPhos and CySPhos, the spectra show two distinct peaks: a broad singlet and a sharp singlet (Figures 12 and 13). For CySPhos, the peak at ca. 38 ppm is likely the $Pd(CySPhos)_2$ complex,[37] while the peak at ca. 44 ppm is likely the Pd(CySPhos) complex.[38] These data imply that under standard cross-coupling conditions, both PdL_1 and PdL_2 complexes are present. Moreover, the peak that is tentatively assigned as the Pd(CySPhos) complex is also observed during kinetic monitoring of the oxidative addition of *p*-chloroanisole to CySPhos-supported palladium complexes. In addition, the amount of free ligand also increases. These observations support the hypothesis that oxidative addition of *p*-chloroanisole undergoes oxidative addition to two distinct species. These kinetic data, presented in the SI (section 8), provide little useful information regarding reaction rates.

With regard to reductive elimination, it has been suggested that increasing the electron-donating ability of the phosphine will retard reductive elimination by electronically stabilizing

DOI: 10.1021/acs.organomet.9b00153
Organometallics XXXX, XXX, XXX−XXX

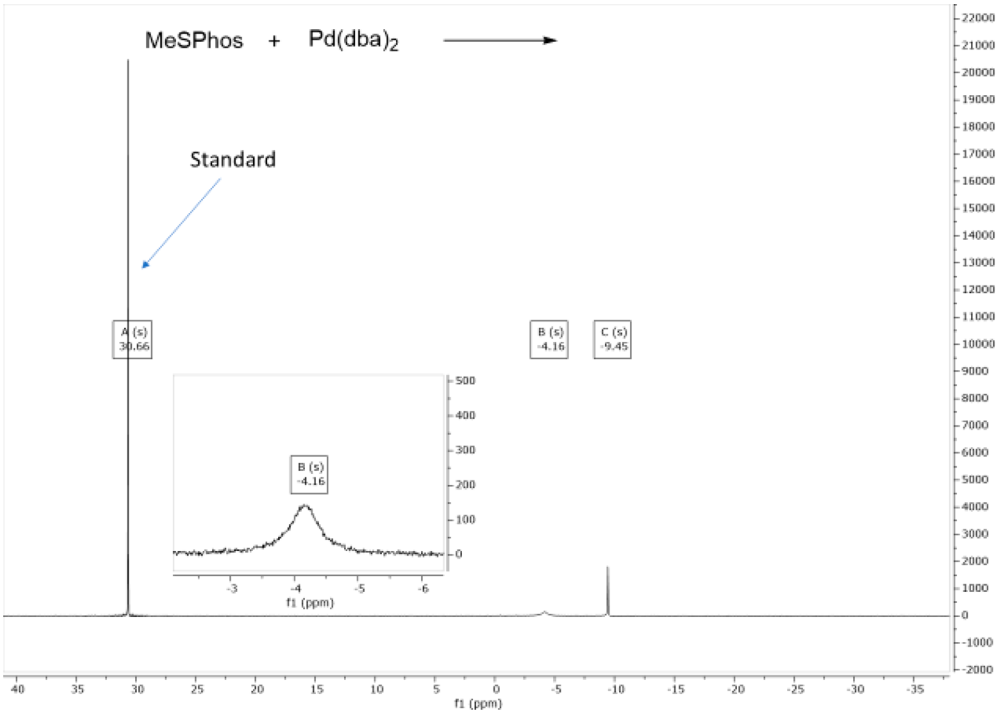

Figure 13. ^{31}P $\{^{1}H\}$ NMR spectrum of the reaction between MeSPhos and $Pd(dba)_2$ in dioxane. The broad singlet at ca. −4 ppm and sharp singlet at ca. −9 are hypothesized to be PdL_1 and PdL_2 species; however, definitive assignments have not been made.

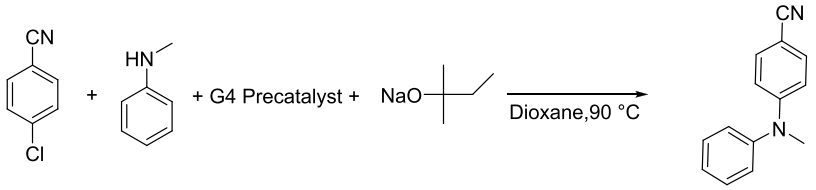

Figure 14. Palladium-catalyzed amination of *p*-chlorobenzonitrile with *N*-methylaniline was chosen as a model reaction to study the rate of cross-coupling. In this instance, the precatalyst was used to avoid problems with delayed catalyst activation. *N*-Methylaniline was chosen as the amine because it is conveniently monitored by NMR and is comparable in cross-coupling properties to morpholine. [ArCl] = 0.25 M, [Amine] = 0.30 M, [Base] = 0.35 M.

the amine-bound oxidative addition complex.[5] However, past studies on analogous palladium-catalyzed etherification reactions by Hartwig and co-workers suggest that the rate of reductive elimination is determined primarily by the ligand's steric bulk and only slightly by the ligand's electronic properties.[39] For the reactions in this study, it was not possible to attribute the difference in reductive elimination rates to differences in the sterics or the electronics of the ligands because of the significant difference between MeSPhos and CySPhos in both sterics and electronics (MeSPhos is an approximately 12% stronger σ donor compared to CySPhos; MeSPhos is 12% smaller than CySPhos). For example, consider the rates of two cross-coupling reactions (Figure 14, SI section 8). The cross-coupling reaction between *p*-chlorobenzonitrile and *n*-methylaniline at 90 °C using MeSPhos reached approximately 50% completion in 150 min (k_{obs} = 3 × 10^{-3} s^{-1}), after which no additional product formed.[40] In contrast, CySPhos reached completion in approximately 10 s (k_{obs} estimated as 4 × 10^{0} s^{-1}). Whether the slower rate for the MeSPhos system is caused by the increased electron-donating ability of this ligand or by its smaller size cannot be determined. These results suggest that it is necessary to tune a ligand for three equally important factors: (1) electron-rich phosphorus to promote oxidative addition; (2) sterically congested phosphorus to promote reductive elimination; and (3) sterically bulky ligand backbone to prevent metallic aggregation. These requirements greatly complicate the process of rational ligand design for this type of catalysis because the most electron-rich phosphine substituents are in general the sterically smallest,[18] implying that there may be a catalytic sweet spot. Furthermore, these requirements suggest that the task of oxidatively adding highly deactived aryl chlorides may remain out of reach until novel phosphines can be designed that are both sterically large and electron rich.

Formation and Decomposition of the Oxidative Addition Complex. As shown in Figures 11 and 15, treatment of a solution of the precatalyst and griseofulvin with sodium *t*-butoxide led to complete and nearly immediate (∼10 min) activation of the precatalyst and formation of the oxidative addition complex. Addition of the sodium *t*-butoxide caused a color change to red then deep black. The ^{31}P NMR spectrum displayed a single major peak, which was unique compared to the spectrum obtained from activating the precatalyst with sodium *t*-butoxide in the absence of any aryl chloride. Subsequent treatment of the reaction mixture with 3-fluoro-*N*-methylaniline led to the rapid precipitation of a black

DOI: 10.1021/acs.organomet.9b00153
Organometallics XXXX, XXX, XXX−XXX

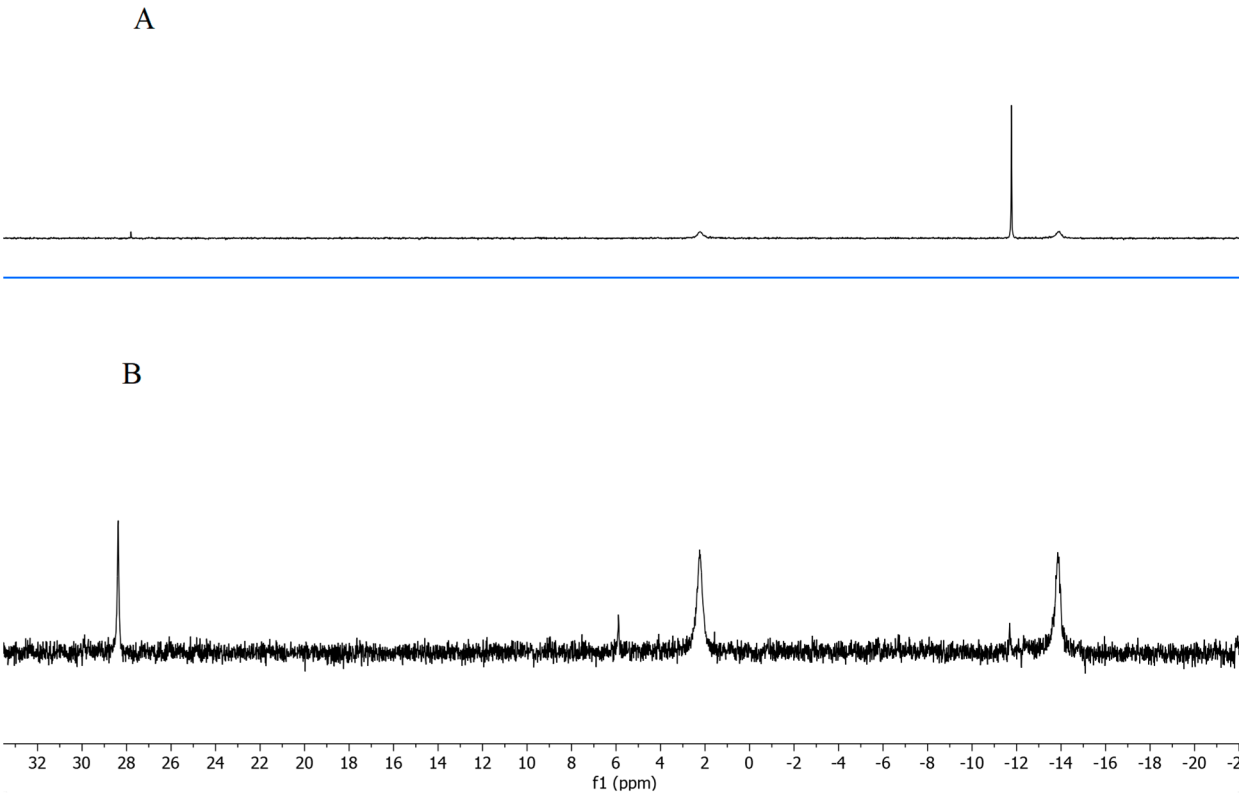

Figure 15. ^{31}P $\{^{1}H\}$ NMR spectrum of the stepwise cross-coupling of griseofulvin with 3-fluoro-*N*-methylaniline using MeSPhos Pd G4 precatalyst. Spectrum A shows the formation of the oxidative addition complex with griseofulvin (ca. −11 ppm). Spectrum B, enormously magnified compared to spectrum A, is the reaction solution immediately after addition of 3-fluoro-*n*-methylaniline. The precatalyst appears at −8 ppm and is absent in both spectra. The minor peaks (+28.5, +6, +2, and −14 ppm, respectively) are unidentified decomposition products.

solid that was completely insoluble in all organic and aqueous solvents tested (over 30 in all). The ^{31}P NMR spectrum showed that the dominant peak at ca. −11 ppm, assigned as the oxidative addition complex, disappeared nearly completely.

It is well established that palladium catalysts typically decompose by the formation of palladium aggregates (colloquially referred to as palladium black).[11,41,42] Likewise, it has been proposed that the shielding degree, a particular measure of steric bulk, can predict the stability of mononuclear organometallic complexes.[43] In the case of common dialkylbiaryl phosphine ligands, the ligand supplies adequate steric protection so as to largely prevent metallic aggregation; however, with MeSPhos we postulate that there is insufficient steric bulk to shield the metal center, and thus aggregation of palladium readily occurs. This suggestion is well supported by the steric data reported above, which shows that MeSPhos is unusually small. In consequence, the decomposition of MeSPhos-supported Pd complexes is unusually facile.

Chemical intuition suggests that an additional factor contributes to the instability of the oxidative addition complexes in the MeSPhos system. When MeSPhos is used as a ligand, the oxidative addition product is more electron dense than the analogous complexes with CySPhos due to the greater σ-donating ability of the MeSPhos ligand. The increased electron density in the case of the MeSPhos system may promote metallic aggregation leading to catalyst decomposition. Finally, the data suggest that the electron density of the aryl halide also likely impacts the stability of the oxidative addition complex. In particular, because *p*-chlorobenzonitrile was the sole successful substrate, it is suggested that electron withdrawing halides increase the stability of the oxidative addition complex, giving the reductive elimination reaction a chance to compete with the decomposition reaction. To summarize this section, two factors, low steric bulk and electron-rich oxidative addition complexes, likely contribute to the decomposition of the MeSPhos·Pd oxidative addition complexes on a time scale comparable to reductive elimination.

SUMMARY AND CONCLUSIONS

The rational design and synthesis of a dialkylbiaryl phosphine ligand, MeSPhos, was reported. We hypothesized that this ligand would combine the high σ-donating ability of the related MeJPhos ligand with the high steric bulk of the previously reported and thoroughly utilized CySPhos. MeSPhos was found to be an exceptional electron-donating phosphine which promoted the oxidative addition of aryl chlorides that are not reactive using typical ligands. However, no positive relationship between electron-donating ability and the rates of oxidative addition could be established. In fact, initial data suggests that there may be an inverse relationship. The altered steric and electronic properties of MeSPhos compared to CySPhos had an equally significant impact on the rate of reductive elimination, and the small steric size caused a substantial decrease in the overall stability of the active catalytic species. The instability of the active catalyst explains the low yield in the sole successful C−N cross-coupling reaction as well as the inability of MeSPhos-supported palladium to cross-couple deactivated aryl chlorides with amines; the decomposition reaction rate is far faster than the cross-coupling reaction rate for all but the most activated substrates. These results illustrate

DOI: 10.1021/acs.organomet.9b00153
Organometallics XXXX, XXX, XXX−XXX

two key points: (1) The electron density of the phosphine influences the ability to oxidatively add challenging aryl chlorides, but changing the electron density has a complex effect on the rate thereof; and (2) although the commercially available CySPhos ligand cannot promote the oxidative addition of highly deactived aryl chlorides, it possesses steric and electronic parameters optimal to promoting both the oxidative addition and reductive elimination steps in the catalytic cycle.

EXPERIMENTAL SECTION

General Considerations. Unless otherwise noted, all reactions were run in oven-dried glassware under an inert atmosphere of nitrogen utilizing standard Schlenk techniques or in a drybox maintained at less than 2 ppm of O_2. Diethyl ether and tetrahydrofuran (THF) were dried using a DriSolv system using CuO and molecular sieves under argon. Other solvents were purified according to literature procedures and distilled under nitrogen.[44] Amines were purchased from TCI and purified by passing through a column of activated and dry alumina before storage under nitrogen in a drybox. All other reagents were used as received. Thin layer chromatography (TLC) was visualized with long-wavelength ultraviolet light and phosphomolybdic acid. NMR spectra were recorded on a 500 MHz INOVA-500, a 500 MHz Avance-500 Bruker, or a 600 MHz Avance-600 Bruker spectrometer and reported relative to the internal solvent signal for proton and carbon spectra, or relative to the external standard (85% H_3PO_4 in D_2O) for phosphorus. All spectra were collected at 25 °C unless otherwise noted. The results are reported as chemical shift (δ, ppm), multiplicity, coupling constant (Hz), and relative integration. Infrared spectra were recorded using a Nicolet Magna-550 Fourier transform infrared spectrophotometer using an air-free fluorite prism solution cell with a 0.1 mm cell thickness.

Synthesis of 2′-(Dimethyl phosphine oxide)-2,6-dimethoxy 1,1′-biphenyl (3). An oven-dried 100 mL Schlenk round-bottom flask was charged with **2** (1.6 g, 4.567 mmol), 50 mL dry degassed tetrahydrofuran, and sodium triflate (2.357 g, 13.701 mmol). A water-cooled reflux condenser was attached and the reaction mixture was cooled to 0 °C. A recirculator was attached to the reflux condenser and set to 0 °C, the temperature of which was confirmed before continuing. A freshly titrated 0.63 M solution of methyl magnesium bromide in diethyl ether (18.1 mL, 11.417 mmol) was slowly added dropwise down the reflux condenser in such a way that the drops were precooled and dripped off the lip of the condenser. The reaction mixture was stirred under nitrogen for 20 min at room temperature before being heated to reflux. After 2 h of refluxing, the reaction mixture was cooled to room temperature. The reaction was subsequently quenched by pouring it into a separatory funnel charged with 100 mL 0.5 M sulfuric acid in water. The layers were quickly separated. (Note this must be done quickly to prevent polymerization of the tetrahydrofuran.) The aqueous layer was washed 5 times with 25 mL dichloromethane. The combined organic layers were dried over sodium sulfate. The mixture was filtered and solvent removed under reduced pressure to yield a yellow oil. A short (ca. 7 cm) plug of silica in a 30 mm flash chromatography column was loaded with ethyl acetate. The oil was wet loaded in ethyl acetate and washed with 100 mL ethyl acetate and subsequently with 100 mL isopropanol. The solvent was removed from the isopropanol fraction under reduced pressure and the oil dried under high vacuum to yield a hydroscopic colorless glass, yield = 0.9423 g, 71%. ^{1}H NMR (500 MHz, $CDCl_3$) δ 8.29 (dd, J = 12.6, 7.2 Hz, 1H), 7.56 (t, J = 7.4 Hz, 1H), 7.55−7.47 (m, 1H), 7.36 (t, J = 8.5 Hz, 1H), 7.16−7.09 (m, 1H), 6.62 (d, J = 8.4 Hz, 1H), 3.68 (s, 5H), 1.32 (d, J = 13.4 Hz, 5H). ^{31}P {^{1}H} NMR (202 MHz, $CDCl_3$) δ 34.67. ^{13}C NMR (126 MHz, $CDCl_3$) δ 157.95, 136.47 (d, J = 10.4 Hz), 134.54, 133.77, 132.97 (d, J = 7.4 Hz), 131.66 (d, J = 10.5 Hz), 131.52 (d, J = 2.4 Hz), 118.33 (d, J = 3.4 Hz), 103.78, 55.48, 17.70 (d, J = 70.6 Hz).

Synthesis of MeSPhos (4). A 100 mL two-neck Schlenk flask was charged with 8 mL dry degassed tetrahydrofuran and a stir bar. **3** (2.4158 g, 8.32 mmol) was added to the solvent by syringe. An addition funnel was attached to one neck and a rubber septum to the other neck. The addition funnel was charged with 30 mL dry degassed tetrahydrofuran and diisobutylaluminum hydride (4.1515 g, 29.17 mmol) was transferred by cannula to the addition funnel. The flask was cooled to 0 °C and the diisobutylaluminum hydride added dropwise with strong stirring. The flask was stirred at 0 °C for 15 min before the ice bath was removed and the addition funnel quick-switched for a reflux condenser attached to a recirculator set at 5 °C. The reaction was heated to reflux for 4 h. After 4 h, the flask was cooled to room temperature. The reaction mixture was transferred by cannula to a 500 mL Schlenk flask. A solution of sodium tribasic phosphate 12-hydrate (32 g, 84 mmol) in 350 mL distilled, sparged water was added by cannula slowly while cooling the reaction mixture to 0 °C with strong stirring. The resulting homogeneous mixture was allowed to stir at room temperature for 4 h. Degassed pentane, 20 mL, was added by syringe and the flask thoroughly mixed by vigorous shaking. The layers were allowed to separate without stirring and the organic layer extracted using a syringe before being transferred to a 250 mL Schlenk flask. This extraction technique was repeated 4 times. Dichloromethane was then added to the crude reaction mixture and the extraction procedure repeated three times. From both the hexane extracts and the dichloromethane extracts, the solvent was removed under high vacuum with gentle heating to yield a white solid. Both fractions were transferred to a glovebox maintained at less than 2 ppm oxygen. The hexane extract was taken up in approximately 5 mL diethyl ether and forced through a pipet packed with basic alumina. An additional 5 mL of diethyl ether was pushed through the column and both fractions combined, and the solvent removed to yield a white solid (1.8296 g, 72%). The phosphine can be further purified by recrystallization with hexane if necessary. The dichloromethane extracts were found to contain nearly exclusively phosphine oxide (**3**) which is easily purified by taking up into isopropanol and pushing through silica to yield the pure phosphine oxide, which can be reused for subsequent reductions. ^{1}H NMR (500 MHz, $CDCl_3$) δ 7.65−7.60 (m, 1H), 7.50−7.41 (m, 2H), 7.30−7.25 (m, 1H), 7.25−7.20 (m, 1H), 6.67 (d, J = 8.1 Hz, 1H), 6.57 (d, J = 8.3 Hz, 1H), 3.72 (s, 3H), 1.16 (dd, J = 35.0, 3.4 Hz, 7H). ^{31}P {^{1}H} NMR (202 MHz, $CDCl_3$) δ −51.69. ^{13}C NMR (126 MHz, benzene-d_6) δ 158.46, 142.68 (d, J = 15.4 Hz), 140.54 (d, J = 30.1 Hz), 131.50 (d, J = 5.3 Hz), 129.19, 129.00 (d, J = 1.4 Hz), 128.18, 127.52, 104.05, 67.15, 55.21, 14.74 (d, J = 15.4 Hz).

In Situ Synthesis of (MeSPhos)Cr(CO)$_5$. In a nitrogen filled glovebox, a 20 mL scintillation vial was charged with chromium hexacarbonyl (21.8 mg, 99.1 μmol) **Caution: toxic!** and MeSPhos (28.0 mg, 102 μmol). Dry, degassed tetrahydrofuran (10 mL) was added. A small portion was transferred by syringe into a CaF_2 cell and the cell was removed from the glovebox. Before irradiation, an IR spectrum was acquired. The sample was then irradiated using a high-pressure mercury arc lamp and the spectra immediately recorded. The sample was observed to turn pale yellow after approximately 5 min of irradiation. Irradiation times required for definitive assignment may depend on the intensity of irradiation; however, in our experience irradiation times of 10, 30, 90, 180, and 600 s (total times) were sufficient to observe conversion of the chromium hexacarbonyl into the monosubstituted species and subsequent conversion to the *trans*-disubstituted species. From each spectrum, the cell filled with only THF was subtracted and the baseline corrected.

In Situ Synthesis of (CySPhos)Cr(CO)$_5$. The above procedure was used; however, CySPhos was used in lieu of MeSPhos, and the UV intensity of the mercury arc lamp was reduced by placing a borosilicate glass beaker in front of the IR cell.

Synthesis of trans-(MeSPhos)$_2$Pd(Cl)$_2$. In a nitrogen filled glovebox, a 25 mL round-bottom flask was charged with $PdCl_2$ (59.1 mg, 0.333 mmol) and MeSPhos (181.9 mg, 0.663 mmol). Dry, degassed dichloromethane (8 mL) was added with a Teflon coated stir bar. The heterogeneous mixture was stirred vigorously for 24 h, after which it was a homogeneous pale yellow solution. The solution was filtered through Celite, washed with 2 mL dichloromethane, and the solvent removed under reduced pressure to yield a yellow powder.

DOI: 10.1021/acs.organomet.9b00153
Organometallics XXXX, XXX, XXX−XXX

The powder was triturated 3 times with 1 mL diethyl ether to yield the title compound as a light yellow solid. Crystals suitable for X-ray crystallography were grown by vapor diffusion using THF/Pentane. Yield = 136.6 mg (57%). ^{1}H NMR (500 MHz, benzene-d_6) δ 8.44 (q, J = 6.9 Hz, 1H), 7.21−7.07 (m, 5H), 6.36 (d, J = 8.2 Hz, 2H), 3.29 (s, 6H), 1.52 (t, J = 3.6 Hz, 6H). ^{31}P {^{1}H} NMR (202 MHz, benzene-d_6) δ −4.11. ^{13}C NMR (126 MHz, benzene-d_6) δ 158.69, 139.06, 135.47 (t, J = 8.2 Hz), 133.93, 132.87 (t, J = 3.5 Hz), 129.81 (d, J = 34.7 Hz), 127.01 (d, J = 5.7 Hz), 119.28, 103.83, 100.37, 55.07, 13.27 (t, J = 15.4 Hz). (Note that in $CDCl_3$ this compound is in equilibrium with a dimer, resulting in two peaks at −3.2 and 9.50 ppm.)

Synthesis of Chloro(2-dimethylphosphino-2′,6′-dimethoxy-1,1′-biphenyl)(2′-amino-1,1′-biphenyl-2-yl)palladium(II) (5). In a nitrogen filled glovebox, a 20 mL scintillation vial was charged with (2′-methylamino-1,1′-biphenyl-2-yl)methanesulfonatopalladium-(II) dimer (559.6 mg, 0.7291 mmol) and MeSPhos (4) (400 mg, 1.458 mmol). Dry, degassed dichloromethane (17 mL) was added with a Teflon coated stir bar. The black solution was allowed to stir under nitrogen for 1.5 h. The solvent was then removed with the use of a rotary evaporator, cold pentane was added, and the heterogeneous mixture filtered using a glass frit. The solids were washed sequentially with 10 mL diethyl ether, then methyl *tert*-butyl ether. The purified precatalyst was collected by washing the frit with 100 mL dichloromethane and removing the solvent under high vacuum. Crystals suitable for X-ray crystallography were grown by vapor diffusion using $CDCl_3$/diethyl ether. ^{1}H NMR (500 MHz, $CDCl_3$) δ 8.02 (dd, J = 13.2, 7.8 Hz, 1H), 7.55 (t, J = 7.6 Hz, 1H), 7.52−7.42 (m, 2H), 7.37 (t, J = 8.4 Hz, 1H), 7.31 (d, J = 6.8 Hz, 1H), 7.22−7.17 (m, 1H), 7.11 (s, 0H), 7.04 (s, 1H), 6.77 (s, 1H), 6.65 (t, J = 9.2 Hz, 2H), 3.72 (s, 6H), 1.32 (d, J = 11.1 Hz, 3H), 1.05 (d, J = 9.8 Hz, 3H). ^{31}P {^{1}H} NMR (202 MHz, $CDCl_3$) δ 8.17. ^{13}C NMR (151 MHz, methylene chloride-d_2) δ 158.54, 158.19, 145.29 (d, J = 4.4 Hz), 142.85 (d, J = 3.3 Hz), 141.60, 140.01 (d, J = 6.8 Hz), 138.74, 137.54 (d, J = 13.6 Hz), 134.87 (d, J = 15.5 Hz), 133.34 (d, J = 7.3 Hz), 132.22, 131.92, 131.04 (d, J = 2.7 Hz), 130.48, 129.26, 128.53, 127.75 (d, J = 11.4 Hz), 127.39 (d, J = 4.7 Hz), 127.03 (d, J = 9.4 Hz), 125.74, 122.61 (d, J = 2.7 Hz), 118.21 (d, J = 4.0 Hz), 104.36 (d, J = 26.5 Hz), 67.59, 55.98 (d, J = 20.3 Hz), 40.35 (d, J = 2.5 Hz), 39.94, 15.29 (d, J = 34.5 Hz), 13.89 (d, J = 29.8 Hz).

General Procedure for MeSPhos-Catalyzed Aminations. In a nitrogen filled glovebox, an unregulated pressure vessel was charged with the appropriate aryl chloride (1 equiv, 1 mmol), dioxane (4 mL), the appropriate amine (1.2 mmol), and sodium *tert*-pentoxide (1.4 mmol). The precatalyst (0.04 mmol, 4% loading) was added as a stock solution in dioxane. A Teflon coated stir bar was added, and the vessel sealed and removed from the glovebox. The vessel was heated to 90 °C in an oil bath behind a blast resistant shield for 20 h with strong stirring, during which time an extremely dark red color developed. The vessel was removed from the oil, diluted with diethyl ether, and filtered through a pad of Celite. Reaction outcome was determined by comparison of the proton NMR spectrum to previously published results. Crude reactions were further analyzed by GC-MS and ^{15}N/^{1}H HMBC. Yields are estimated based on recovered mass and corrected for purity as determined by GCMS/^{1}H NMR.

In Situ Formation of Oxidative Addition Complexes for Kinetic Analysis. To a J-Young adapted NMR tube in a nitrogen filled glovebox was added the appropriate phosphine (2.0 equiv, 25 μmol). The aryl chloride, *p*-chloroanisole (32 μL, 250 μmol), was added by syringe. Dioxane (68 μL) was added by syringe. A sealed capillary tube containing the internal standard, tetraethyl-1,2-ethanebisphosphonate in C_6D_6 was added. Palladium(dba)$_2$ (7.2 mg, 12.5 μmol) was added as a solution in dioxane (400 μL). The tube was then quickly removed from the glovebox and inserted into the instrument. The time in all experiments is the time from palladium addition. See SI for details on quantitative ^{31}P NMR.

In Situ Formation of Active Catalysts Using Pd(dba)$_2$. To a J-Young adapted NMR tube in a nitrogen filled glovebox was added the appropriate phosphine (2.0 equiv, 0.25 μmol). Dioxane (68 μL) was added by syringe. A sealed capillary tube containing the internal standard, tetraethyl-1,2-ethanebisphosphonate in C_6D_6 was added. Palladium(dba)$_2$ (7.2 mg, 12.5 μmol) was added as a solution in dioxane (400 μL). The tube was then quickly removed from the glovebox and inserted into the instrument.

Stoichiometric Cross-Coupling of Griseofulvin and 3-Fluoro-*N*-methylaniline. In a nitrogen filled glovebox a 1 dram vial was charged with MeSPhos Pd G4 precatalyst **5** (21 mg, 31.86 μmmol), griseofulvin (9.5 mg, 26.9 μmol), and 600 μL of d_8-tetrahydrofuran. Sodium *tert*-pentoxide (4.9 mg, 41 μmol) was added resulting in an immediate change to a copper color. The reaction mixture was taken up into a syringe and filtered with a 0.2 μm syringe filter directly into a J-Young adapted NMR tube. The tube was sealed and removed from the glovebox and an NMR spectrum collected. The reaction was returned to the glovebox and 3-fluoro *n*-methylaniline (7.5 mg, 69.99 μmol) was added by syringe. An additional amount (1.8 mg, 16.34 μmol) of sodium *tert*-pentoxide was added and the reaction sealed and removed from the glovebox. Addition of the amine resulted in an immediate color change to black along with precipitation of a black solid. An NMR spectrum was subsequently obtained.

Kinetics of Cross-Coupling Reaction. In a nitrogen filled glovebox, a 20 mL scintillation vial was charged with a Teflon coated stir bar and charged with *p*-chlorobenzonitrile (137.57 mg, 1.0 mmol), hexamethylbenzene internal standard (28 mg, 0.17 mmol), *N*-methylaniline (129 μL 1.2 mmol), and the appropriate precatalyst (0.022 mmol). Dioxane (2 mL) was then added. A solution of sodium *tert*-pentoxide (154.2 mg, 1.4 mmol) was prepared in 2.0 mL dioxane. The reaction mixture was heated to 90 °C in an oil bath, and the sodium *tert*-pentoxide added by syringe. Aliquots (400 μL) were taken by syringe and quenched by addition to 2 mL methanol. The solvent was then removed under reduced pressure with gentle heating and dried on high vacuum. (*Note: the starting material may be volatile depending on pressure and temperature, and so integrals of starting material may be inaccurate if a consistent solvent removal protocol is not followed. The product is not volatile and not subject to the same variability.)* The time in all experiments is the time when the base was added. See SI for details on quantitative ^{1}H NMR.

X-ray Crystallography. Diffraction intensities for precatalyst **5** and $PdCl_2$(MeSPhos)$_2$ were collected at 173 K, respectively, on a Bruker Apex2 CCD diffractometer using Cu Kα radiation, λ = 1.54178 Å. Space groups were determined based on systematic absences ($PdCl_2$(MeSPhos)$_2$) and intensity statistics (**5**). Absorption corrections were applied by SADABS.[45] Structures were solved by direct methods and Fourier techniques and refined on F^2 using full matrix least-squares procedures. All non-H atoms were refined with anisotropic thermal parameters. H atoms in all structures were refined in calculated positions in a rigid group model. Solvent molecules Et_2O in precatalyst **5** fill out empty space around an inversion center and are highly disordered. This solvent molecule was treated by SQUEEZE;[46] corrections of the X-ray data by SQUEEZE is 28 electron/cell. The crystal structure of $PdCl_2$(MeSPhos)$_2$ seems to have orthorhombic pseudosymmetry based on symmetry of the central heavy atoms fragment, but the structure was solved and refined in a monoclinic crystallographic system. All calculations were performed by the Bruker SHELXL-2014 package.[47]

The X-ray crystallographic data for molecule **5** and $PdCl_2$(MeSPhos)$_2$ have been deposited at the Cambridge Crystallographic Data Centre (CCDC) under deposition numbers CCDC 1895567 and CCDC 1895568, respectively. These data can be obtained free of charge from the CCDC (www.ccdc.cam.ac.uk/data_request/cif).

■ ASSOCIATED CONTENT

Supporting Information

The Supporting Information is available free of charge on the ACS Publications website at DOI: 10.1021/acs.organomet.9b00153.

Additional discussion of general considerations, additional syntheses, and commentary on procedures,

DOI: 10.1021/acs.organomet.9b00153
Organometallics XXXX, XXX, XXX−XXX

infrared and NMR spectra and detailed kinetics plots (PDF)

Accession Codes

CCDC 1895567−1895568 contain the supplementary crystallographic data for this paper. These data can be obtained free of charge via www.ccdc.cam.ac.uk/data_request/cif, or by emailing data_request@ccdc.cam.ac.uk, or by contacting The Cambridge Crystallographic Data Centre, 12 Union Road, Cambridge CB2 1EZ, UK; fax: +44 1223 336033.

AUTHOR INFORMATION

Corresponding Author

*E-mail: dtyler@uoregon.edu.

ORCID

David R. Tyler: 0000-0002-5032-7533

Notes

The authors declare no competing financial interest.

ACKNOWLEDGMENTS

Acknowledgment is made to the NSF (CHE-1503550) for the support of this research.

REFERENCES

(1) Torborg, C.; Beller, M. Recent Applications of Palladium-Catalyzed Coupling Reactions in the Pharmaceutical, Agrochemical, and Fine Chemical Industries. *Adv. Synth. Catal.* **2009**, *351* (18), 3027−3043.

(2) Bariwal, J.; van der Eycken, E. C−N Bond Forming Cross-Coupling Reactions: An Overview. *Chem. Soc. Rev.* **2013**, *42* (24), 9283−9303.

(3) Guram, A. S.; Renells, R. A.; Buchwald, S. L. A Simple Catalytic Method for the Conversion of Aryl Bromides to Arylamines - Guram - 1995 - Angewandte Chemie International Edition in English - Wiley Online Library. *Angew. Chem., Int. Ed. Engl.* **1995**, *34* (12), 1348−1350.

(4) Louie, J.; Hartwig, J. F. Palladium-Catalyzed Synthesis of Arylamines from Aryl Halides. Mechanistic Studies Lead to Coupling in the Absence of Tin Reagents. *Tetrahedron Lett.* **1995**, *36* (21), 3609−3612.

(5) Surry, D. S.; Buchwald, S. L. Dialkylbiaryl Phosphines in Pd-Catalyzed Amination: A User's Guide. *Chem. Sci.* **2011**, *2* (1), 27−50.

(6) Ruiz-Castillo, P.; Buchwald, S. L. Applications of Palladium-Catalyzed C−N Cross-Coupling Reactions. *Chem. Rev.* **2016**, *116* (19), 12564−12649.

(7) Christmann, U.; Vilar, R. Monoligated Palladium Species as Catalysts in Cross-Coupling Reactions. *Angew. Chem., Int. Ed.* **2005**, *44* (3), 366−374.

(8) Barrios-Landeros, F.; Carrow, B. P.; Hartwig, J. F. Effect of Ligand Steric Properties and Halide Identity on the Mechanism for Oxidative Addition of Haloarenes to Trialkylphosphine Pd(0) Complexes. *J. Am. Chem. Soc.* **2009**, *131* (23), 8141−8154.

(9) Bruno, N. C.; Niljianskul, N.; Buchwald, S. L. N-Substituted 2-Aminobiphenylpalladium Methanesulfonate Precatalysts and Their Use in C−C and C−N Cross-Couplings. *J. Org. Chem.* **2014**, *79* (9), 4161−4166.

(10) Barder, T. E.; Biscoe, M. R.; Buchwald, S. L. Structural Insights into Active Catalyst Structures and Oxidative Addition to (Biaryl)-Phosphine−Palladium Complexes via Density Functional Theory and Experimental Studies. *Organometallics* **2007**, *26* (9), 2183−2192.

(11) Iwasawa, T.; Tokunaga, M.; Obora, Y.; Tsuji, Y. Homogeneous Palladium Catalyst Suppressing Pd Black Formation in Air Oxidation of Alcohols. *J. Am. Chem. Soc.* **2004**, *126* (21), 6554−6555.

(12) Viciu, M. S.; Kelly, R. A.; Stevens, E. D.; Naud, F.; Studer, M.; Nolan, S. P. Synthesis, Characterization, and Catalytic Activity of N-Heterocyclic Carbene (NHC) Palladacycle Complexes. *Org. Lett.* **2003**, *5* (9), 1479−1482.

(13) Zhang, Y.; César, V.; Storch, G.; Lugan, N.; Lavigne, G. Skeleton Decoration of NHCs by Amino Groups and Its Sequential Booster Effect on the Palladium-Catalyzed Buchwald−Hartwig Amination. *Angew. Chem., Int. Ed.* **2014**, *53* (25), 6482−6486.

(14) Weber, P.; Scherpf, T.; Rodstein, I.; Lichte, D.; Scharf, L. T.; Gooßen, L. J.; Gessner, V. H. A Highly Active Ylide-Functionalized Phosphine for Palladium-Catalyzed Aminations of Aryl Chlorides. *Angew. Chem., Int. Ed.* **2019**, *58* (10), 3203−3207.

(15) Harkal, S.; Rataboul, F.; Zapf, A.; Fuhrmann, C.; Riermeier, T.; Monsees, A.; Beller, M. Dialkylphosphinoimidazoles as New Ligands for Palladium-Catalyzed Coupling Reactions of Aryl Chlorides. *Adv. Synth. Catal.* **2004**, *346* (13−15), 1742−1748.

(16) Schwarz, N.; Pews-Davtyan, A.; Michalik, D.; Tillack, A.; Krüger, K.; Torrens, A.; Diaz, J. L.; Beller, M. Palladium-Catalyzed Amination and Sulfonylation of 5-Bromo-3-[2-(Diethylamino)-Ethoxy]Indoles to Potential 5-HT6 Receptor Ligands. *Eur. J. Org. Chem.* **2008**, *2008* (32), 5425−5435.

(17) Driver, M. S.; Hartwig, J. F. A Second-Generation Catalyst for Aryl Halide Amination: Mixed Secondary Amines from Aryl Halides and Primary Amines Catalyzed by (DPPF)PdCl2. *J. Am. Chem. Soc.* **1996**, *118* (30), 7217−7218.

(18) Kendall, A. J.; Zakharov, L. N.; Tyler, D. R. Steric and Electronic Influences of Buchwald-Type Alkyl-JohnPhos Ligands. *Inorg. Chem.* **2016**, *55* (6), 3079−3090.

(19) Kendall, A. *Synthesis, Study, and Catalysis of the New Dimethyl-Phosphine Ligands*; University of Oregon: Eugene, OR, 2016.

(20) Kendall, A. J.; Salazar, C. A.; Martino, P. F.; Tyler, D. R. Direct Conversion of Phosphonates to Phosphine Oxides: An Improved Synthetic Route to Phosphines Including the First Synthesis of Methyl JohnPhos. *Organometallics* **2014**, *33* (21), 6171−6178.

(21) Rinehart, N. I.; Kendall, A. J.; Tyler, D. R. A Universally Applicable Methodology for the Gram-Scale Synthesis of Primary, Secondary, and Tertiary Phosphines. *Organometallics* **2018**, *37* (2), 182−190.

(22) Cotton, F. A.; Kraihanzel, C. S. Vibrational Spectra and Bonding in Metal Carbonyls. I. Infrared Spectra of Phosphine-Substituted Group VI Carbonyls in the CO Stretching Region. *J. Am. Chem. Soc.* **1962**, *84* (23), 4432−4438.

(23) Atkins, P.; Overton, T. *Shriver and Atkins' Inorganic Chemistry*; OUP Oxford, 2010.

(24) Graham, W. A. G. Approach to the Separation of Inductive and Mesomeric Effects in Complexes of the Types LMn(CO)5 and LMo(CO)5 - Inorganic Chemistry (ACS Publications. *Inorg. Chem.* **1968**, *7* (2), 315−321.

(25) Falivene, L.; Credendino, R.; Poater, A.; Petta, A.; Serra, L.; Oliva, R.; Scarano, V.; Cavallo, L. SambVca 2. A Web Tool for Analyzing Catalytic Pockets with Topographic Steric Maps. *Organometallics* **2016**, *35* (13), 2286−2293.

(26) Starosta, R.; Baźanów, B.; Barszczewski, W. Chalcogenides of the Aminomethylphosphines Derived from 1-Methylpiperazine, 1-Ethylpiperazine and Morpholine: NMR, DFT and Structural Studies for Determination of Electronic and Steric Properties of the Phosphines. *Dalton Trans.* **2010**, *39* (32), 7547−7555.

(27) Xu, C.; Li, Y.-F.; Wang, Z.-Q.; Cen, F.-F.; Zhang, Y.-Q. Dibromidobis[2-(Dicyclohexylphosphanyl)biphenyl-KP]Palladium-(II). *Acta Crystallogr., Sect. E: Struct. Rep. Online* **2008**, *64* (10), m1349−m1349.

(28) Barder, T. E.; Walker, S. D.; Martinelli, J. R.; Buchwald, S. L. Catalysts for Suzuki−Miyaura Coupling Processes: Scope and Studies of the Effect of Ligand Structure. *J. Am. Chem. Soc.* **2005**, *127* (13), 4685−4696.

(29) Kashin, A. S.; Ananikov, V. P. Catalytic C−C and C−Heteroatom Bond Formation Reactions: In Situ Generated or Preformed Catalysts? Complicated Mechanistic Picture Behind Well-Known Experimental Procedures. *J. Org. Chem.* **2013**, *78* (22), 11117−11125.

DOI: 10.1021/acs.organomet.9b00153
Organometallics XXXX, XXX, XXX−XXX

(30) Viciu, M. S.; Grasa, G. A.; Nolan, S. P. Catalytic Dehalogenation of Aryl Halides Mediated by a Palladium/Imidazolium Salt System. *Organometallics* **2001**, *20* (16), 3607−3612.
(31) de Vries, J. G. A Unifying Mechanism for All High-Temperature Heck Reactions. The Role of Palladium Colloids and Anionic Species. *Dalton Trans.* **2006**, No. 3, 421−429.
(32) Ananikov, V. P.; Beletskaya, I. P. Toward the Ideal Catalyst: From Atomic Centers to a "Cocktail" of Catalysts. *Organometallics* **2012**, *31* (5), 1595−1604.
(33) Strieter, E. R.; Blackmond, D. G.; Buchwald, S. L. Insights into the Origin of High Activity and Stability of Catalysts Derived from Bulky, Electron-Rich Monophosphinobiaryl Ligands in the Pd-Catalyzed C−N Bond Formation. *J. Am. Chem. Soc.* **2003**, *125* (46), 13978−13980.
(34) Brazier, J. B.; Newton, M. A.; Barreiro, E. M.; Adrio, L. A.; Naya, L.; Hii, K. K. (Mimi). Solvent-Dependent Nuclearity, Geometry and Catalytic Activity of [(SPhos)Pd(Ph)Cl]2. *Dalton Trans.* **2017**, *46* (22), 7223−7231.
(35) Definitive conclusions about the relative rates of the two reactions could not be drawn because practical technical difficulties prevented us from acquiring data during the first 30 minutes of the reaction. Numerous attempts to work around this technical difficulty proved fruitless..
(36) We attempted to use the generation four precatalysts for oxidative addition kinetics, but the data was not suitable for publication due to irreproducibility. The initial data did, however, suggest two mechanisms were occurring..
(37) Reid, S. M.; Boyle, R. C.; Mague, J. T.; Fink, M. J. A Dicoordinate Palladium(0) Complex with an Unusual Intramolecular η-Arene Coordination. *J. Am. Chem. Soc.* **2003**, *125* (26), 7816−7817.
(38) There is no evidence that the $Pd^0(PR_3)_2(n^2\text{-dba})$ complex (PR_3 = MeSPhos or CySPhos) forms in any detectable amount.[18,48].
(39) Mann, G.; Shelby, Q.; Roy, A. H.; Hartwig, J. F. Electronic and Steric Effects on the Reductive Elimination of Diaryl Ethers from Palladium(II). *Organometallics* **2003**, *22* (13), 2775−2789.
(40) The amination of *p*-chlorobenzonitrile with *N*-methylaniline at 90 °C was chosen because it was the sole reaction for which MeSPhos successfully promoted cross-coupling..
(41) van Leeuwen, P. W. N. M. Decomposition Pathways of Homogeneous Catalysts. *Appl. Catal., A* **2001**, *212* (1), 61−81.
(42) Tromp, M.; Sietsma, J. R. A.; van Bokhoven, J. A.; van Strijdonck, G. P. F.; van Haaren, R. J.; van der Eerden, A. M. J.; van Leeuwen, P. W. N. M.; Koningsberger, D. C. Deactivation Processes of Homogeneous Pd Catalysts Using in Situ Time Resolved Spectroscopic Techniques. *Chem. Commun.* **2003**, *0* (1), 128−129.
(43) Zakharov, L. N.; Saf'yanov, Yu. N.; Domrachev, G. A. A Role of Non-Bonding Interactions in the Chemistry of Organometalic Compounds. *Inorg. Chim. Acta* **1989**, *160* (1), 77−82.
(44) Armarego, W. L. F.; Chai, C. *Purification of Laboratory Chemicals - 6th ed.*, 6th ed.; Elsevier, 2009.
(45) Sheldrick, G. M. *G. M. Bruker/Siemens Area Detector Absorption Correction Program, SADABS*; Bruker AXS Inc: Madison, Wisconsin, USA, 1998.
(46) van der Sluis, P.; Spek, A. L. BYPASS: An Effective Method for the Refinement of Crystal Structures Containing Disordered Solvent Regions. *Acta Crystallogr., Sect. A: Found. Crystallogr.* **1990**, *46* (3), 194−201.
(47) Sheldrick, G. M. Crystal Structure Refinement with SHELXL. *Acta Crystallogr., Sect. C: Struct. Chem.* **2015**, *71* (1), 3−8.
(48) Majchrzak, M.; Kostera, S.; Kubicki, M.; Kownacki, I. Synthesis of New Styrylarenes via Suzuki−Miyaura Coupling Catalysed by Highly Active, Well-Defined Palladium Catalysts. *Dalton Trans.* **2013**, *42* (44), 15535−15539.

DOI: 10.1021/acs.organomet.9b00153
Organometallics XXXX, XXX, XXX−XXX